TCAD Modeling for Si–Ge HBT THz Detectors

Xueqing Liu, John Suarez, and Michael Shur

Abstract – Terahertz (THz) response of transistor and integrated circuit yields important information about device parameters and has been used for distinguishing between working and defective transistors and circuits. Using a technology computer-aided design (TCAD) model for Si–Ge heterojunction bipolar transistors (HBTs), we simulate the current–voltage characteristics and the response to sub-THz (300 GHz) radiation. Applying different mixed mode schemes in TCAD, we simulated the dynamic range of the THz response for Si–Ge HBTs and showed that it is comparable with that of the field effect transistor–based THz (TeraFET) detectors. The HBT response to the variations of the detector design parameters are investigated at different frequencies with the harmonic balance simulation in TCAD. These results are useful for the physical design and optimization for the HBT THz detectors and for the identification of faulty Si–Ge HBT and Si bipolar (Bi)CMOS circuits by using sub-THz or THz scanning.

1. Introduction

Emerging beyond 5G communications and many other subterahertz and terahertz (THz) applications, communications, scanning, testing, biologic, medical, and industrial control have stimulated the demand for efficient sub-THz and THz detectors [1–6]. Plasmonic field effect transistor–based THz (TeraFETs) implemented in In–Ga–As, Ga–As, Ga–N, and Si have demonstrated efficient detection on the basis of the excitation of decayed plasm waves [7–11]. The InP heterojunction bipolar transistors (HBTs) have also demonstrated a reasonable performance in detecting THz radiation [12, 13]. Si–Ge HBTs and bipolar (Bi)CMOS circuits, which are compatible with standard very large-scale integration (VLSI) technology, have shown advantages for many applications [14–17].

In this article, we report on the modeling of the Si–Ge HBTs for THz detection. The dynamic range of the Si–Ge HBT response has been simulated and compared with various TeraFET detectors. The Si–Ge HBT response to the variations of the device feature size ranging from 20 nm to 130 nm and other design parameters are explored for such detectors. These results could be important for testing Si BiCMOS VLSI by using THz scanning.

Manuscript received 2 June 2020.

Xueqing Liu and Michael Shur are with Department of Electrical, Computer, and Systems Engineering, Rensselaer Polytechnic Institute, 110 Eighth Street, Troy, NY 12180, USA; e-mail: liux29@rpi.edu, shurm@rpi.edu.

John Suarez is with Electrical Engineering Department, Widener University, One University Place, Chester, PA 19013, USA; e-mail: jsuarez@widener.edu.

2. Model Setup

Figure 1 shows the structure of the Si–Ge HBT in Synopsys Sentaurus technology computer-aided design (TCAD). The model is set up to simulate a double-polysilicon self-aligned Si–Ge HBT with an emitter area of 0.13 $\mu m^2 \times 2.73\ \mu m^2$ [18, 19]. Default material parameters for Si and Si–Ge in Sentaurus are used for the TCAD model. The model accounts for the physical mechanisms, including the hydrodynamic transport, velocity saturation, and generation recombination [20]. For the boundary conditions, the emitter, base, and collector contacts are set as ohmic contacts. The device parameters in the TCAD model are tuned to fit the measured I–V characteristics [19]. Table 1 summarizes the adjusted device parameters. Figure 2 shows good agreement between the simulated results and measured data.

3. Response Simulation Approach

For the modeling of THz detection, we ran mixed mode simulations in Sentaurus with the TCAD model. We also include the validated TeraFET TCAD models for comparison [21, 22]. Figure 3 shows the two schemes of the mixed mode simulations in Sentaurus. The schematic in Figure 3a is the typical configuration illustrated for theoretic analysis of the THz response, in which the THz signal is not modulated. This configuration could be simulated with either transient or harmonic balance (HB) simulations in Sentaurus. For the transient simulation, the THz voltage response at the collector or the drain could be extracted from the Fourier transform of the collector or drain voltage waveform at the zero frequency or dc component. For the HB simulation, the THz voltage response could be

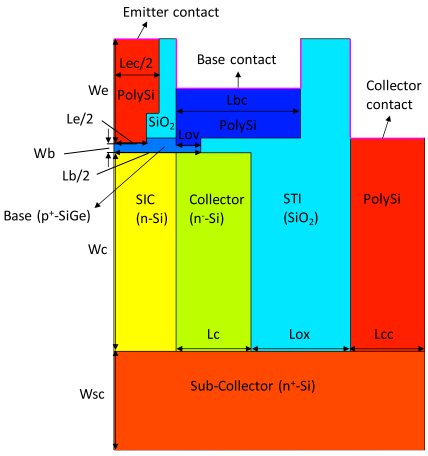

Figure 1. Schematic of the Si–Ge HBT structure in TCAD.

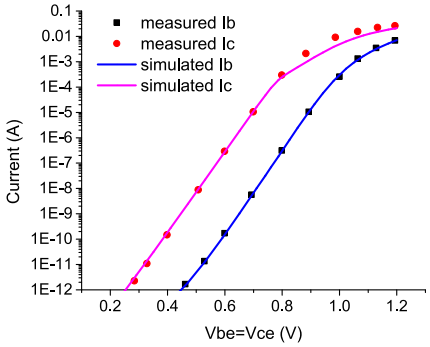

Figure 2. Comparison of the simulated I–V characteristics with the measured data [19].

simply extracted from the zero or dc component of the collector or drain voltage when the simulation is completed. The schematic in Figure 3b is the typical configuration used in practical measurements, where the THz signal V_a is modulated by another ac voltage source V_m with a modulation frequency f_m much lower than the THz signal frequency f. This configuration could only be simulated with the time-varying transient simulation in Sentaurus. The THz response could also be extracted from the Fourier transform of the collector or drain voltage waveform but at the modulation frequency f_m.

The time-varying schemes with or without modulation have been validated in [22]. To evaluate the HB scheme, we use the silicon-on-insulator (SOI) MOSFET TeraFET TCAD model in [22]. Figure 4 shows the comparison of the simulated drain response as a function of the THz signal magnitude for the SOI

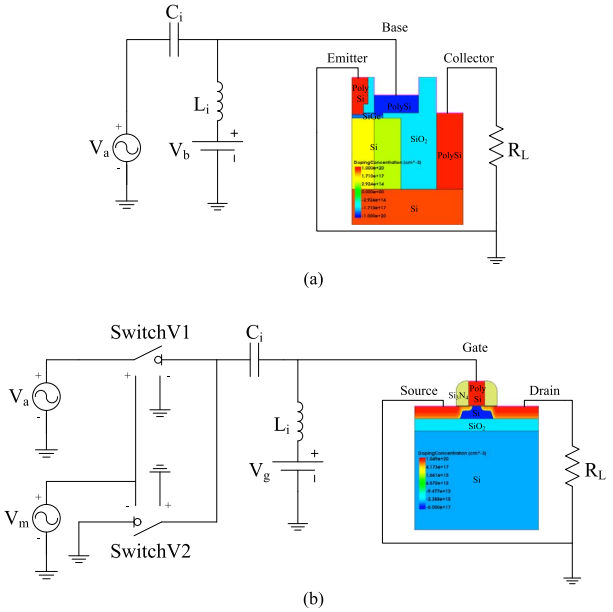

Figure 3. Schematics of mixed mode simulation for THz detection with the TCAD models (a) without modulation and (b) with modulation.

Table 1. Summary of the device parameters for the Si–Ge HBT TCAD model

Series device parameters	Series value
Emitter width We (μm)	0.21
Base width Wb (μm)	0.02
Collector width Wc (μm)	0.4
Subcollector width Wsc (μm)	0.2
Emitter length Le (μm)	0.13
Base length Lb (μm)	0.35
Collector length Lc (μm)	0.15
Emitter contact length Lec (μm)	0.18
Base contact length Lbc (μm)	0.15
Collector contact length Lcc (μm)	0.15
Si–Ge and Base PolySi overlap Lov (μm)	0.05
Shallow trench isolation Lox (μm)	0.2
PolySi doping (cm^{-3})	1e20
Base doping (cm^{-3})	3e18
SIC doping (cm^{-3})	1e16
Collector doping (cm^{-3})	1e15
Subcollector doping (cm^{-3})	2e19

MOSFET model. The response of the transient simulation without modulation is extracted from the waveform with the time range between $20/f$ and $50/f$. The transient simulation results with and without modulation are in good agreement, and the results with modulation deviate from the quadratic response (proportional to V_a^2) due to the nonideal voltage-controlled switches in Figure 3b. This is consistent with the results of the Al–Ga–As–In–Ga–As HFET in [22]. Also, the HB simulation results agree with the transient simulation results without modulation, which validates the HB approach for THz response simulation in Sentaurus. At high THz signal magnitude, the HB simulation suffers from convergence problems, and transient simulation could be used.

The different schemes are then applied to the Si–Ge HBT TCAD simulations. Figure 5 shows the dependence of the simulated response on the THz signal magnitude for the Si–Ge HBT model. For the transient simulation scheme without modulation, different time ranges for the collector voltage wave-

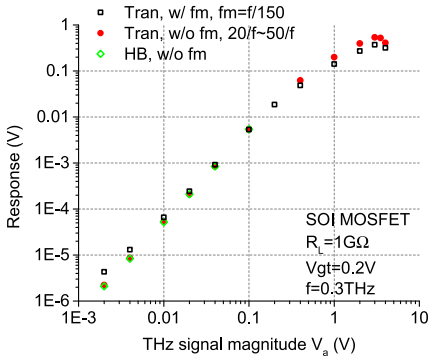

Figure 4. Simulated drain response at 0.3 THz as a function of the THz signal magnitude for the SOI MOSFET TCAD model with different schemes.

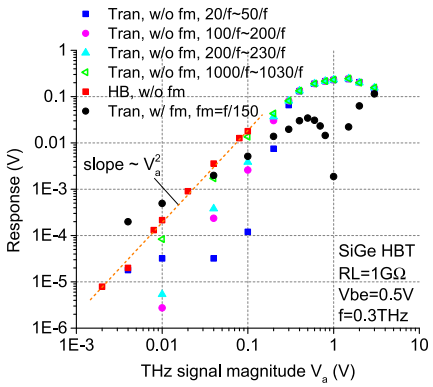

Figure 5. Simulated collector response at 0.3 THz as a function of the THz signal magnitude for the Si–Ge HBT TCAD model with different schemes.

form are used for the extraction of the THz response. The comparison shows that the time-varying simulation with modulation may not be proper for the Si–Ge HBT response simulation, because the HBT may not have large enough input impedance to minimize the influence of the nonideal voltage-controlled switches. Also, the time range of the collector voltage waveform for the THz response extraction from the Fourier transform could have a significant effect on the results at the low or medium V_a ranges. The longer time the transient simulation takes, the more accurate results are obtained because they are becoming closer to the HB simulation results that could be considered the correct results. At high intensities ($V_a > 0.2$ V), however, the results are the same for different time ranges used for the response extraction. This suggests an efficient simulation approach for the Si–Ge HBT response, which is to use HB simulations in the low and intermediate V_a ranges and transient simulation without modulation in the high V_a range. The results also show the quadratic response at the low and medium intensity range and the response saturation at the high intensity range for the Si–Ge HBT, which is consistent with the V_a dependence of the response for the TeraFET detectors [22].

4. Response Simulation Results

Using the proposed scheme, we obtain the dynamic range of the THz response for the Si–Ge HBT model and compare the results with the TeraFET TCAD models in [22]. Figure 6 shows the comparison of the THz response and responsivity. The responsivity as a function of the power for the TCAD models is calculated by normalizing the simulated response as a function of the THz signal magnitude to the measured responsivity for Si MOSFETs in [23]. The modeling results are obtained by using the transient simulation without modulation, except for the Si–Ge HBT model in the 1 mV and 0.1 V range of the THz signal magnitude, where the response is obtained from the HB simulation. These devices have comparable dynamic ranges, and Si–Ge HBTs could work as efficient THz detectors as the TeraFETs implemented in different material systems.

The mixed mode HB simulation could be a very useful tool for the physical design of the THz detector, because it runs much faster than the time-varying transient simulation. By running the HB simulation at the intermediate V_a range, we explore the Si–Ge HBT response to the variations of the device design parameters at different frequencies. Figure 7 shows the simulated results for various base parameter

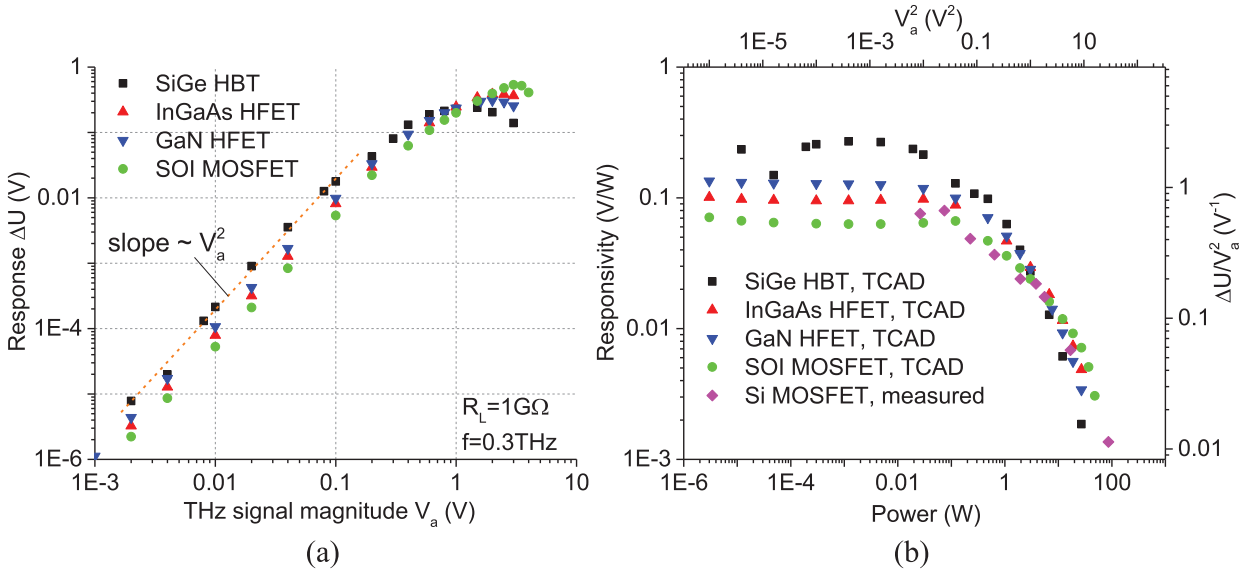

Figure 6. Comparison of the dynamic ranges: (a) simulated collector or drain response for the Si–Ge HBT and TeraFET TCAD models and (b) simulated responsivity normalized to the measured data [23].

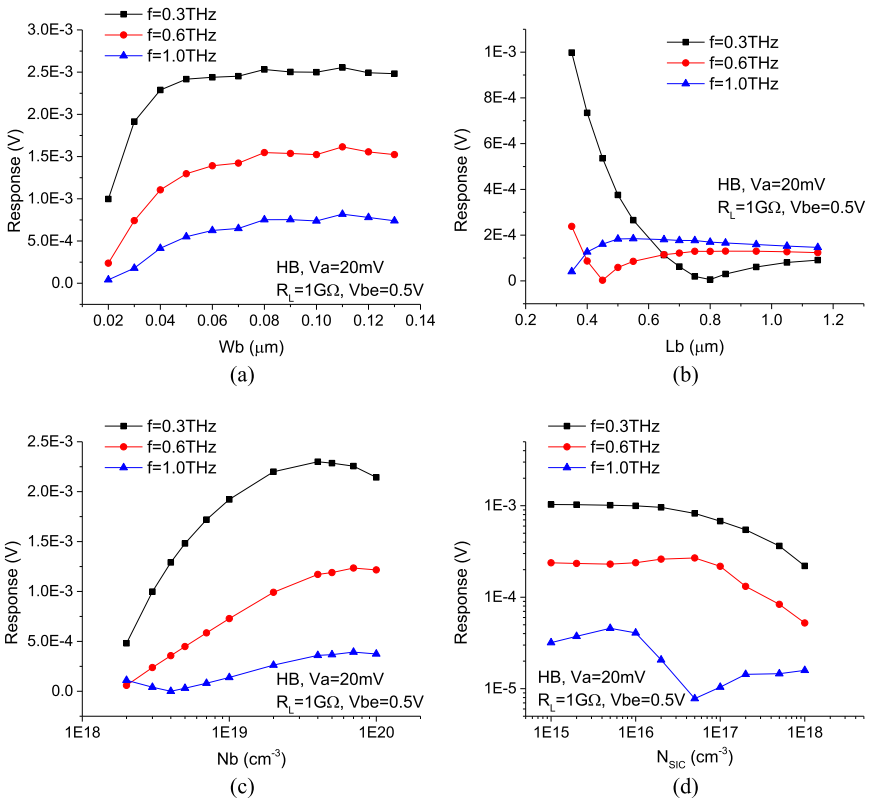

Figure 7. Simulated collector response to the variations of the device design parameters for the Si–Ge HBT TCAD model at different frequencies.

values, including the width, length, and doping, as well as the collector doping values. Therefore, high detector response could be obtained by optimizing the device parameters, such as adopting medium base width, small base length, high base doping, and low selectively implanted collector (SIC) doping. These results also suggest an effective approach of using THz scanning to test Si BiCMOS VLSI, because the THz response could be different between the working and defective devices or the authentic and counterfeit chips.

5. Conclusion

The TCAD model for the Si–Ge HBT detector is in good agreement with the measured current–voltage characteristics and shows the quadratic response at the low and medium intensity ranges and the response saturation at the high intensity range. The dynamic range is comparable with the dynamic range of the various TeraFET detectors. The mixed mode HB simulation for the Si–Ge HBT response to the variations of the device parameters provides an efficient approach for the detector design and optimization. The simulation results could be applied in the nondestructive testing of Si BiCMOS VLSI with THz radiation.

6. References

1. M. A. Akkas, “Terahertz Wireless Data Communication,” *Wireless Networks*, **25**, 1, January 2019, pp. 145-155.
2. G. Klatt, R. Gebs, C. Janke, T. Dekorsy, and A. Bartels, “Rapid-Scanning Terahertz Precision Spectrometer With More Than 6 THz Spectral Coverage,” *Optics Express*, **17**, 25, December 2009, pp. 22847-22854.
3. J. F. Federici, B. Schulkin, F. Huang, D. Gary, R. Barat, et al., “THz Imaging and Sensing for Security Applications—Explosives, Weapons and Drugs,” *Semiconductor Science and Technology*, **20**, 7, June 2005, pp. S266-S280.
4. H. Cheon, H.-j. Yang, S.-H. Lee, Y. A. Kim, and J.-H. Son, “Terahertz Molecular Resonance of Cancer DNA,” *Scientific Reports*, **6**, November 2016, p. 37103, doi: 10.1038/srep37103.
5. L. Xie, W. Gao, J. Shu, Y. Ying, and J. Kono, “Extraordinary Sensitivity Enhancement by Metasurfaces in Terahertz Detection of Antibiotics,” *Scientific Reports*, **5**, March 2015, p. 8671, doi: 10.1038/srep08671.
6. K. Ahi, S. Shahbazmohamadi, and N. Asadizanjani, “Quality Control and Authentication of Packaged Integrated Circuits Using Enhanced-Spatial-Resolution Terahertz Time-Domain Spectroscopy and Imaging,” *Optics and Lasers in Engineering*, **104**, May 2018, pp. 274-284, doi: 10.1016/j.optlaseng.2017.07.007.
7. M. I. Dyakonov and M. S. Shur, “Detection, Mixing, and Frequency Multiplication of Terahertz Radiation by Two-Dimensional Electronic Fluid,” *IEEE Transactions on Electron Devices*, **43**, 3, March 1996, pp. 380-387.
8. M. I. Dyakonov and M. S. Shur, “Plasma Wave

Electronics: Novel Terahertz Devices Using Two-Dimensional Electron Fluid," *IEEE Transactions on Electron Devices*, **43**, 10, October 1996, pp. 1640-1645.
9. V. V. Popov, D. M. Ermolaev, K. V. Maremyanin, N. A. Maleev, V. E. Zemlyakov, et al., "High-Responsivity Terahertz Detection by On-Chip InGaAs/GaAs Field-Effect-Transistor Array," *Applied Physics Letters*, **98**, 15, April 2011, p. 153504.
10. V. Gavrilenko, E. Demidov, K. Marem'yanin, S. Morozov, W. Knap, et al., "Electron Transport and Detection of Terahertz Radiation in a GaN/AlGaN Submicrometer Field-Effect Transistor," *Semiconductors*, **41**, 2, February 2007, pp. 232-234.
11. W. Knap, F. Teppe, Y. Meziani, N. Dyakonova, J. Lusakowski, et al., "Plasma Wave Detection of Sub-Terahertz and Terahertz Radiation by Silicon Field-Effect Transistors," *Applied Physics Letters*, **85**, 4, July 2004, pp. 675-677.
12. D. Coquillat, V. Nodjiadjim, S. Blin, A. Konczykowska, N. Dyakonova, et al., "High-Speed Room Temperature Terahertz Detectors Based on InP Double Heterojunction Bipolar Transistors," *International Journal of High Speed Electronics and Systems*, **25**, 03n04, December 2016, p. 1640011.
13. N. Dyakonova, D. Coquillat, D. B. But, F. Teppe, W. Knap, et al., "Detection of High Intensity THz Radiation by InP Double Heterojunction Bipolar Transistors," 42nd International Conference of Infrared, Millimeter, Terahertz Waves, Cancun, Mexico, September 2017, pp. 1-2.
14. A. Mai, I. Garcia Lopez, P. Rito, R. Nagulapalli, A. Awny, et al., "High-Speed SiGe BiCMOS Technologies and Circuits," *International Journal of High Speed Electronics and Systems*, **26**, 01n02, June 2017, p. 1740002.
15. M. Schröter, T. Rosenbaum, P. Chevalier, B. Heinemann, S. P. Voinigescu, et al., "SiGe HBT Technology: Future Trends and TCAD-Based Roadmap," *Proceedings of the IEEE*, **105**, 6, January 2016, pp. 1068-1086.
16. R. Al Hadi, J. Grzyb, B. Heinemann, and U. Pfeiffer, "Terahertz Detector Arrays in a High-Performance SiGe HBT Technology," IEEE Bipolar/BiCMOS Circuits and Technology Meeting, Portland, OR, October 2012, pp. 1-4.
17. H. Ghodsi and H. Kaatuzian, "Analysis and Design of a SiGe-HBT Based Terahertz Detector for Imaging Arrays Applications," *Microelectronics Journal*, **90**, June 2019, pp. 156–162, doi: 10.1016/j.mejo.2019.06.007.
18. P. Chevalier, T. F. Meister, B. Heinemann, S. Van Huylenbroeck, W. Liebl, et al., "Towards THz SiGe HBTs," IEEE Bipolar/BiCMOS Circuits and Technology Meeting, Atlanta, GA, October 9–11, 2011, pp. 57-65.
19. J. Böck, K. Aufinger, S. Boguth, C. Dahl, H. Knapp, et al., "SiGe HBT and BiCMOS Process Integration Optimization Within the DOTSEVEN Project," IEEE Bipolar/BiCMOS Circuits and Technology Meeting, Boston, MA, October 25–28, 2015, pp. 121-124.
20. Synopsys Inc. *Sentaurus Device User Guide (Version N-2017.09)*, Mountain View, Synopsys Inc., 2017.
21. X. Liu and M. Shur, "An Efficient TCAD Model for TeraFET Detectors," IEEE Radio and Wireless Symposium, Orlando, FL, May 16, 2019, pp. 1-4.
22. X. Liu and M. Shur, "TCAD Model for TeraFET Detectors Operating in a Large Dynamic Range," *IEEE Transactions on Terahertz Science and Technology*, **10**, 1, January 2020, pp. 15-20.
23. P. Zagrajek, S. N. Danilov, J. Marczewski, M. Zaborowski, C. Kolacinski, et al., "Time Resolution and Dynamic Range of Field-Effect Transistor–Based Terahertz Detectors," *Journal of Infrared, Millimeter, and Terahertz Waves*, **40**, 7, July 2019, pp. 703-719.